A robust scheme for free surface and pressurized flows in channels with arbitrary cross-sections

ELISA ALDRIGHETTI, Ph. D. Student, Department of Mathematics, University of Trento, Via Sommarive 14, I-38050 Povo (Trento), Italy

GUUS STELLING, Full Professor, Fluid Mechanics Section, Faculty of Civil Engineering and Geosciences, Technical University of Delft, P.O. Box 5084,2600 GA Delft, The Netherlands.

SUMMARY

Flows in closed channels often contain transitions from free surface to pressurized flows, or vice versa. These phenomena usually require two different sets of equations for the two different flow regimes. Actually, a few specifications for the geometry of the channel and for the discretization choices can be sufficient to model closed channel flows using the open channel flow equations. Transitions can also occur in open channels, like those from super to subcritical flows, or vice versa. These flows are usually difficult to treat numerically and strong restrictions are imposed to simulate them. A semi-implicit finite volume conservative model is proposed to deal with these problems and a special flux limiter is implemented to allow accurate flow simulations near hydraulic structures such as weirs. Some computational examples are given to illustrate the properties of the scheme and the numerical solutions are compared with experimental data, when possible.

KEY WORDS: Saint Venant equations; free surface flow; pressurized flow; transitions; hydraulic jumps; flux limiter

Introduction

The transition from free surface to pressurized flow or vice versa is a phenomenon often occurring in closed

This situation may happen for example in storm sewers systems during heavy storm events or even in a closed channel with initially free surface flow as a result of the start-up of machinery (turbines, pumps, gates).

Because of the wide range of practical problems involving closed channel flows, numerical methods are needed to predict the water profile, pressure and discharge during pipes pressurization and depressurization.

The one-dimensional equations for free surface as well as pressurized flows in closed channels are essentially the Saint Venant Equations:

$$(1.1) A_t + Q_x = 0$$

(1.1)
$$A_t + Q_x = 0$$

$$(1.2) \qquad Q_t + (UQ)_x + gA\eta_x + c_f \frac{|U|}{R_H} Q = 0$$

where U is the cross-sectional averaged water velocity, η is the water level for free surface flows and the pressure head for pressurized flows measured vertically from a reference datum, $A(x, \eta(x, t))$ is an arbitrary but prescribed function of space and water surface elevation representing the cross-section area and Q = AU is the discharge; g is the gravitational constant, c_f is a non-negative friction coefficient (see, e.g., Reference [3] for the definition) and R_H is the hydraulic radius. Moreover, $H = \eta + h$, where H is the total water depth and h is the depth below reference plane.

Two types of algorithms broadly used in the literature for the numerical solution of the Saint Venant Equations are the explicit [4, 5, 8] and the implicit ones [2, 10].

In the present paper, the performance of the numerical scheme presented in Reference [1] is investigated for the simulation of free surface as well as pressurized flows in closed channels. This technique is semi-implicit in time, fully water volume conservative, satisfies a correct momentum balance near large gradients and deals properly with problems presenting flooding and drying.

In case of closed channel flow the fully implicit version of this technique will be considered here. This time discretization is chosen because unconditionally stable methods, unlike explicit methods, are able to simulate the transition from free surface to pressurized flow in channels with closed sections without any approximation of the section geometry. In fact, assuming the incompressibility of water, they can manage instantaneous transmission of pressure and velocity changes arising in the pressurized part of the channel.

This paper is organized in 5 sections. In Section 2 a brief description of the numerical scheme for the discretization of the Equations (1.1) and (1.2) is given. A special flux limiter function is presented in Section 3 to face the problem of low resolution in case of critical flows and a test to verify its behaviour is also shown. Section 4 gives a few specifications for the geometry of the channel and for the discretization choices in order to model closed channel flows using only the open channel flow equations. Finally, the numerical scheme is validated simulating a flow in a horizontal and downwardly inclined pipe and comparing the numerical results with the experimental data obtained in the laboratory.

2 Numerical method

Equations (1.1) and (1.2) are discretized in the spatial interval [0,L] on a space staggered grid whose nodes are denoted by x_i and $x_{i+1/2}$, i = 0, N + 1. The discrete discharge $Q_{i+1/2}$ (or the velocity $U_{i+1/2}$) is defined at half integer nodes and the discrete variable η_i , representing the water level for free surface flows and the pressure head for pressurized flows, is defined at integer nodes as well as the cross-sectional area A_i and the bottom h_i .

A semi-implicit discretization in time is chosen in order to obtain an efficient and stable numerical method able to cope with free surface flows as well as with pressurized flows.

Specifically, the continuity Equation (1.1) is integrated in time to obtain

$$(2.1) V_i(\eta_i^{n+1}) = V_i(\eta_i^n) - \Delta t \theta [Q_{i+1/2}^{n+\theta} - Q_{i-1/2}^{n+\theta}]$$

where $V_i(\eta_i) = \int_{x_{i-1/2}}^{x_{i+1/2}} Adx$ is, in general, a non linear function of η representing the volume occupied by the water [1] and $Q^{n+\theta} = \theta Q^{n+1} + (1-\theta)Q^n$.

Moreover, the scheme for the momentum Equation (1.2) is the following

$$(2.2) (1 + c_f \frac{|U|_{i+1/2}^n}{R_H} \Delta t) Q_{i+1/2}^{n+1} + g A_{i+1/2}^n \theta \frac{\Delta t}{\Delta x_{i+1/2}} (\eta_{i+1}^{n+\theta} - \eta_i^{n+\theta}) = F_{i+1/2}^n$$

where $F_{i+1/2}^n$ is a finite difference operator including the explicit discretizations of the advective and the free surface (or pressure head) slope terms [1].

From the point of view of the spatial discretization, the discharge is defined as $Q_{i+1/2} = A_{i+1/2}U_{i+1/2}$.

Therefore, remembering that the cross sectional area A, the variable η and the bottom h are initially defined at integers nodes, it is necessary to define explicitly their value at the half integer node i + 1/2.

To do this, the following upwind rule based on the sign of the momentum $Q_{i+1/2}$ is used for the definition of η

(2.3)
$$\eta_{i+1/2} = \begin{cases} \eta_i & \text{if } Q_{i+1/2} \ge 0 \\ \eta_{i+1} & \text{if } Q_{i+1/2} < 0 \end{cases},$$

while the value of the bottom $h_{i+1/2}$ is given by $h_{i+1/2} = max(h_i, h_{i+1})$, except for the case we can analytically express it as $h_{i+1/2} = h(x_{i+1/2})$.

3 A flux limiter for critical flows

A special flux limiter function has been constructed to be used in the extrapolation of the value $\eta_{i+1/2}$ in case of critical flows and it is given, assuming positive flow direction, by the following relation

(3.1)
$$\Psi_{i+1/2} = \Psi(x_{i+1/2}) = \min(0, \max(\frac{-\eta_i/3}{\eta_{i+1} - \eta_i}, 1))$$

One can show that $0 \le \Psi_{i+1/2} \le 1$, that means that a data reconstruction using Ψ defined in (3.1) is consistent, because it is a Total Variation Non Increasing (TVNI) scheme, as stated in the Harten's Theorem [6].

In particular, the reconstruction of η in the node i + 1/2 can be expressed as

(3.2)
$$\eta_{i+1/2} = \min(\eta_i, \max(\frac{2}{3}\eta_i, \eta_{i+1})).$$

The derivation of this special flux limiter follows from the analysis of the specific energy head function [3] in case of a constant discharge $E = H + \frac{U^2}{2g}$. This function assumes its minimum respect to H in the case of critical flows, that is if Fr = 1 ($U = \sqrt{gH}$), and its minimum value is $E = \frac{3}{2}(\frac{Q^2}{gA^2})^{\frac{1}{3}}$, where $H_{cr} = (\frac{U^2}{g})^{\frac{1}{3}}$ is called critical depth. Thus, in case of critical flow, one has $H = \frac{2}{3}E$ (see, e.g., [3]).

Equation (3.2) is finally obtained assuming that the squared velocity is negligible with respect to H and introducing a min-max rule to ensure consistency.

The implementation of this flux limiter improves the accuracy of the method and helps in facing the problems arising in case of low resolution of the grid, as we can show with the following example.

The test presented in this section simulates a steady state problem including a hydraulic jump over a non-flat bed profile in a rectangular frictionless channel.

The domain length is L=100m and in the middle of the channel there is a sill with a crest of 1m height and 10m long and the tangent of the slopes of the sill are abrupt within one grid cell. Moreover, there are two open boundaries, the inflow and the outflow, where a discharge of $1m^3/s$ and a water depth of 1m, respectively, are imposed [9]. The discretization parameters are $c_f = 0$, $g = 9.81m/s^2$, $\theta = 1$ and $\Delta t = 10^{-3}s$.

Figure 1 shows a comparison between the numerical solutions obtained for N = 100 grid points using the flux limiter (3.1) only over the sill (Solution 1) and the numerical solutions obtained for N = 20 grid points with (Solution 2) and without (Solution 3) the help of the flux limiter.

Solutions 1 and 2 are coincident in almost all the nodes in common altough the second grid is five times coarser than the first. Moreover, on equal grid size, the numerical solution obtained using the limiter shows an upstream water level that is consistent with that of Solution 1 and higher than that obtained without the limiter: the reduction of the resolution of the grid causes the upstream water level to decrease in the numerical solution of the first order model.

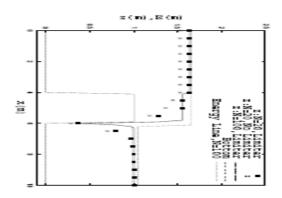


Figure 3.1: High and low resolution grids: effect of the flux limiter

Observe the energy line plotted in Figure 1: as one can see, it is constant everywhere, except near the hydraulic jump where the energy head drops as is to be expected by considerations based on open channel hydraulics [3].

4 Closed channel flow

In order to model closed channel flows using the open channel flow equations, a few specifications for the geometry of the channel, for the physical quantities involved in the problem and for the discretization choices are needed.

In case of free surface flows in a closed channel, as well as for open channel flows, η is the instantaneous water surface elevation measured vertically from a reference datum and assuming an horizontal interface between water and air, the quantities H and A have the usual definitions.

In case of pressurized flows, η plays the role of the pressure head, the water height H is the maximum height reachable $H_{top} = \eta_{top} + h$ and the wetted area A is the area of the whole cross section A_{top} .

Therefore, the total water depth H in a closed channel can be expressed as follows

(4.1)
$$H = \begin{cases} \eta + h & \text{if } \eta \leq \eta_{top} \\ H_{top} & \text{if } \eta > \eta_{top}. \end{cases}$$

while, for the special case of a circular channel with diameter D, the cross-sectional area A is given by

(4.2)
$$A = \begin{cases} \frac{D^2}{4} \left[arccos(1 - \frac{2H}{D}) - (1 - \frac{2H}{D})\sqrt{1 - (1 - \frac{2H}{D})^2} \right] & \text{if } \eta \leq \eta_{top} \\ \pi(D/2)^2 & \text{if } \eta > \eta_{top} \end{cases}$$

The experiments we are going to present have been carried out by the University of Delft and Delft Hydraulics in collaboration with the majority water boards in the Netherlands [7].

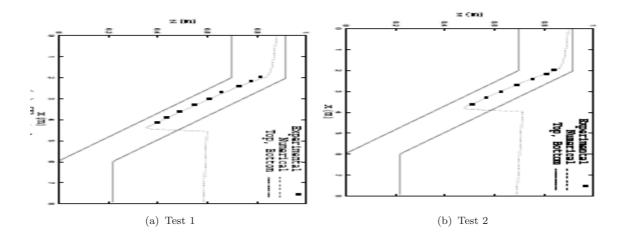
Their aim is the investigation about the air-water phenomena in wastewater pressure mains with respect to transportation and dynamic hydraulic behaviour. Free gas in pressurized pipelines can in fact significantly reduce the flow capacity and may cause undesirable efficiency loss.

The test section of the pipe consists of three parts: a horizontal pipe of length $L_1 = 2m$, a downward inclined pipe ($\alpha = 10^{\circ}$) of length $L_2 = 4m$ and a horizontal pipe of length $L_3 = 2m$. The pipes are circular with an inner diameter of 220mm and are made of transparent material (Perspex with equivalent sand roughness height of $k_s = 0$).

Injecting air into the water and preserving a constant water discharge at the inlet of the pipe and a constant pressure head downstream (Test 1: $Q_{1/2} = 30l/s$ and $\eta = 0.554m$; Test 2: $Q_{1/2} = 45l/s$ and $\eta = 0.69m$), an air pocket appears in the inclined part of the pipe and the obtained configuration presents similarities with hydraulic jumps in open channels.

The numerical results of the present model for the pressure head at the steady state of the phenomenon are compared with the experimental data in Figures 6 and 7. These data are given as measurements of the water depth in a certain number of nodes located along the air pocket at a distance of about 30cm one to the other. The hydraulic jump is located after at most 30cm from the last measurement.

The physical and computational parameters are $q = 9.81 m/s^2$, $\Delta x = 0.06 m$, $\theta = 1$. and $\Delta t = 10^{-2} s$.



5 Conclusions

The performance of the one dimensional, conservative, semi-implicit finite volume model presented in Reference [1] in simulating free surface as well as pressurized flows in channels with arbitrary cross-sections has been investigated. A special flux limiter has been described and implemented to allow accurate flow simulations near hydraulic structures such as weirs, for both critical and subcritical situations including the transition. Some numerical tests have been carried out in order to show the performance of the model. The numerical results have been validated against the experimental data, when possible.

REFERENCES

- 1. Aldrighetti E, Zanolli P. A high resolution scheme for flows in open channels with arbitrary cross-section. *International Journal for Numerical Methods in Fluids*. 2005; **47**:817-824.
- 2. Casulli V, Cattani E. Stability, accuracy and efficiency of a semi-implicit method for three dimensional shallow water flows. Computers & Mathematics with Application. 1994; 15(6):629-648.
- 3. Chanson H. The Hydraulics of Open Channel Flow: An Introduction. 1999; John Wiley & Sons Ltd.
- 4. Cunge J.A, Holly F.M, Verwey A. Practical Aspects of computational river hydraulics. Pitman Publishing, 1980.
- 5. Garcia-Navarro P, Priestley A. An implicit method for water flow modelling in channels and pipes. . *Journal of Hydraulic Research*. 1994; **32**: 721-742.
- 6. Harten A. High resolution schemes for hyperbolic conservation laws. *Journal of Computational Physics*. 1983; **49**: 357-393.
- 7. Lubbers CL, Clemens F.H.L.R. Capacity reduction caused by air intake at wastewater pumping stations. (Experiments of transport of gas in pressurized wastewater mains.) Technical Report, Section of Sanitary Engineering, Faculty of Civil Engineering and Geosciences, Delft University of Technology, The Netherlands, 2005.
- 8. Sjoberg A. Calculation of Unsteady Flows in regulated rivers and Storm Sewer System Division of Hydraulics, Chalmers Univ. of Technology, Goteborg, Sweden, 1976.
- 9. Stelling GS, Duinmeijer SPA. A staggered conservative scheme for every Froude number in rapidly varied shallow water flows. *International Journal for Numerical Methods in Fluids*. 2003; **43**:1329-1354.
- 10. Tucciarelli T. A new algorithm for a robust solution of the fully dynamic Saint-Venant Equations. *Journal of Hydraulic Research*. 2003; **3**:239-243.